

DK-SLAM: Monocular Visual SLAM with Deep Keypoints Adaptive Learning, Tracking and Loop-Closing

Hao Qu, Lilian Zhang, Jun Mao, Junbo Tie, Xiaofeng He, Xiaoping Hu, Yifei Shi, Changhao Chen*

Abstract—Unreliable feature extraction and matching in handcrafted features undermine the performance of visual SLAM in complex real-world scenarios. While learned local features, leveraging CNNs, demonstrate proficiency in capturing high-level information and excel in matching benchmarks, they encounter challenges in continuous motion scenes, resulting in poor generalization and impacting loop detection accuracy. To address these issues, we present DK-SLAM, a monocular visual SLAM system with adaptive deep local features. MAML optimizes the training of these features, and we introduce a coarse-to-fine feature tracking approach. Initially, a direct method approximates the relative pose between consecutive frames, followed by a feature matching method for refined pose estimation. To counter cumulative positioning errors, a novel online learning binary feature-based online loop closure module identifies loop nodes within a sequence. Experimental results underscore DK-SLAM’s efficacy, outperforms representative SLAM solutions, such as ORB-SLAM3 on publicly available datasets.

Index Terms—Monocular SLAM, Deep Learning, Feature Extraction and Matching, Loop Closing.

I. INTRODUCTION

VISUAL localization and mapping constitute crucial components within intelligent mobile agents for motion tracking and environment understanding, with diverse applications ranging from autonomous vehicles, unmanned aerial vehicles (UAVs), and robots to immersive technologies such as Virtual Reality (VR) and Augmented Reality (AR). The imperative nature of achieving robust localization for unmanned platforms across various environmental conditions has garnered escalating attention within the research community.

A Visual Simultaneous Localization and Mapping (SLAM) system comprises front-end perception and back-end optimization. The front-end uses sensors for environmental perception, employing keypoint features in stages like extraction, matching, outlier removal, and pose estimation. The back-end includes loop detection and global map optimization, refining the system state with geometric models. Visual SLAM methods are categorized as keypoint-based and direct methods. Direct methods optimize pixel-level photometric loss but can

be unstable due to lighting variations [1]–[3]. Keypoint-based methods, like ORB-SLAM2 and ORB-SLAM3 [4], [5], enhance stability by using detectors and descriptors, although handcrafted descriptors are susceptible to lighting and texture variations. Addressing these challenges is crucial for improving the reliability of visual localization and mapping systems in diverse applications.

In recent years, deep learning has shown impressive performance in image processing, particularly in image classification and object detection. The application of deep learning to VO/SLAM methods has gained attention, with two predominant approaches: end-to-end and learned features based methods. End-to-end methods utilize Deep Neural Networks (DNNs) to directly convert images into pose estimates [6]. However, they exhibit low interpretability and suboptimal generalization. In contrast, learned-feature-based SLAM replaces local features, allowing deep learning to focus on feature perception [7]–[10]. This approach combines the strengths of deep learning and geometric models but may still face challenges in generalization. Additionally, it may lack crucial low-level keypoint information, impacting feature matching performance. The training complexity of learned-feature-based Bag-of-Words (BoW) adds further challenges, often requiring offline training and exacerbating generalization issues.

To address the aforementioned challenges, we introduce **DK-SLAM**, a novel **Deep Keypoints based SLAM** system incorporating adaptive learning, coarse-to-fine feature tracking, and online loop-closing capabilities. This monocular visual SLAM framework utilizes a modified MAML-based training strategy for robust deep feature extraction. It enhances feature matching precision by incorporating patch pixels and constructs a photometric loss using adjacent frame patches to optimize coarse relative pose estimates. An online BoW model with binary deep features adapts dynamically to new environments, mitigating generalization challenges in deep learning, and improves adaptability without requiring additional training. Our proposed DK-SLAM outperforms the representative baselines, e.g. ORB-SLAM3, LDSO and LIFT-SLAM, on the public KITTI and EuRoC datasets.

Our contributions can be summarized as follows:

- We propose DK-SLAM, a monocular SLAM system with adaptive deep keypoints learning. Our deep feature extractor, trained using a MAML strategy, enhances adaptability to diverse scenes.
- Our method employs a coarse-to-fine feature matching strategy, estimating relative poses through patch photo-

The authors are with the College of Intelligence Science and Technology, National University of Defense Technology, Changsha, 410073, China

*Corresponding author: Changhao Chen (changhao.chen66@outlook.com).

Hao Qu and Lilian Zhang contribute equally to this work.

This work was supported by National Natural Science Foundation of China (NSFC) under the Grant Number of 62103427, 62073331, 62103430, and Major Project of Natural Science Foundation of Hunan Province (No.2021JC0004). Changhao Chen is funded by the Young Elite Scientist Sponsorship Program by CAST (No. YESS20220181)

metric loss optimization and refining them based on the 2D-3D relationship for improved accuracy.

- We introduce an deep keypoints online learning-based Bag-of-Words (BoW) models that overcomes poor generalization, ensuring correct loop detection in the sequence.

II. RELATED WORKS

A. Deep Feature Extractor for Visual SLAM

Mainstream handcrafted extractors, including ORB [11], SIFT [12], and Shi-Thomas [13], are employed in visual SLAMs like ORB-SLAM2 [4] and VINS-Mono [14]. However, these methods relying on gradient information face challenges in dynamic lighting and low-texture environments. To address these issues, researchers explored deep feature extractors. Superpoint [15] employs a shared encoder for high-level information and distinct decoders for keypoints and descriptors, using synthesized labels for self-supervised training. D2-Net [16] eliminates the need for a separate keypoint decoder, ensuring robustness. To enhance repeatability detection, [17] combines multi-scale gradients with depth feature maps. Additionally, L2-Net [18] introduces a local matching loss based on the L2 distance, improving feature matching performance. Experimental results demonstrate the effective feature matching performance of the learned local features on public datasets. Despite their success, the mentioned deep extractors exhibit inherent flaws in the face of diverse scenes, leading to potential performance degradation.

B. Hybrid methods for Visual SLAM

Recent research explores hybrid SLAM methods to combine deep learning and multi-view geometry advantages. GCNv2-SLAM integrates GCN [19] into SLAM, constructing a complete system with offline BoW training. In [20], knowledge distillation from HF-Net [21] enhances feature detection in a compact model. [22] uses a self-supervised thermal optical flow tracking network, while [10] builds on Superpoint [15] with edge and multi-scale information. Our proposed SLAM methodology shares similarities with [8]. In [8], a LIFT [23] extractor serves as the SLAM front-end, implementing an adaptive feature matching strategy tailored to different datasets. In contrast, our SLAM adopts a meta-learning based training strategy, eliminating the need for separate hyperparameter designs for distinct datasets.

C. Loop Closure Module

Loop closure is a critical module of visual SLAM, responsible for detecting loop nodes and refining initial pose estimates. The BoW model, such as DBow2, DBow3, and FBow [24], relies on the binary descriptor BRIEF [25]. DBow utilizes a k-d tree structure based on Hamming distance for descriptor storage. However, conventional BoW methods require extensive offline training data, prompting the introduction of iBow [26]. iBow achieves online word bag training using testing datasets, demonstrating robust transfer performance across various scenarios and addressing adaptability concerns. Another closed-loop detection method, akin to NetVLAD [27] in [9], [20],

is highly reliant on the training set. Substantial differences between test and training sets may result in performance degradation.

III. DEEP KEYPOINT BASED MONOCULAR SLAM

An overview of our proposed DK-SLAM is depicted in Figure 2. We employ an adaptive local feature extractor, based on Superpoint, for extracting keypoints across multi-scale image pyramids. To balance the number of keypoints on varying scale images, we implement an averaging distribution strategy. For enhanced generalization, the local feature extractor undergoes MAML during training. Subsequently, we optimize memory consumption by converting floating descriptors into binary hash codes. Lastly, an online BoW module is introduced to establish a loop closure mechanism, facilitating closed-loop detection and global map optimization.

A. Adaptive Local Feature Learning

1) *Feature Extractor Network*: Inspired by Superpoint, our deep local feature extractor also utilizes VGG16 [28] as the backbone. Different from Superpoint, we introduce BatchNorm layers after each Convolutional Neural Network (CNN) to enhance training convergence. Post the backbone, two heads emerge, each comprising multi-layer CNNs. The first, the detector head, generates a probability mask matching the input image size. We posit that positions with a probability surpassing a set threshold on the mask denote keypoint positions. The second head, the descriptor head, predicts feature descriptors for keypoints, normalized to a dimension of 256 using the L2 norm.

2) *Self-supervised Adaptive Feature Learning*: Our network undergoes self-supervised training, employing a multi-step process. Initially, we obtain the homography-warped image from current training image. To train keypoint detector, we leverage the pre-trained MagicPoint network [15] to acquire keypoint pseudo labels for both the original and warped images. In both images, keypoint predictions and pseudo labels contribute to the formation of detector loss, denoted as L_p and L_{wp} , with CrossEntropy serving as the metric. Moving on to descriptor training, we utilize the sparse descriptor loss L_d proposed in [29]. This involves obtaining both the warped image and pixel-wise correspondences. Descriptor loss functions are then constructed solely for pseudo-labeled keypoints, employing triplet loss. The sparse descriptor loss is composed of two components: homography-matched descriptor loss (L_{dm}) and non-matched descriptor loss (L_{dn}). The homography-matched descriptor loss, represented by Equation 1, involves a subscript i ranging between $(0, 1, \dots, N)$, where $(\mathbf{p}_i, \hat{\mathbf{p}}_i)$ denotes the N matched keypoint position pairs.

$$L_{dm}(\mathbf{p}_i) = \|\mathbf{d}_I(\mathbf{p}_i) - \mathbf{d}_{wI}(\hat{\mathbf{p}}_i)\|^2 \quad (1)$$

As depicted in Equation 2, we use M pairs of descriptors from the vicinity of matched descriptors to formulate a non-matched descriptor loss. The subscript j ranges from 0 to M , where $(\mathbf{p}_i, \mathbf{p}'_j)$ represents unmatched keypoint position pairs.

$$L_{dn}(\mathbf{p}_i) = \frac{1}{M} \sum_{j=1}^M (\|\mathbf{d}_I(\mathbf{p}_i) - \mathbf{d}_{wI}(\mathbf{p}'_j)\|^2) \quad (2)$$

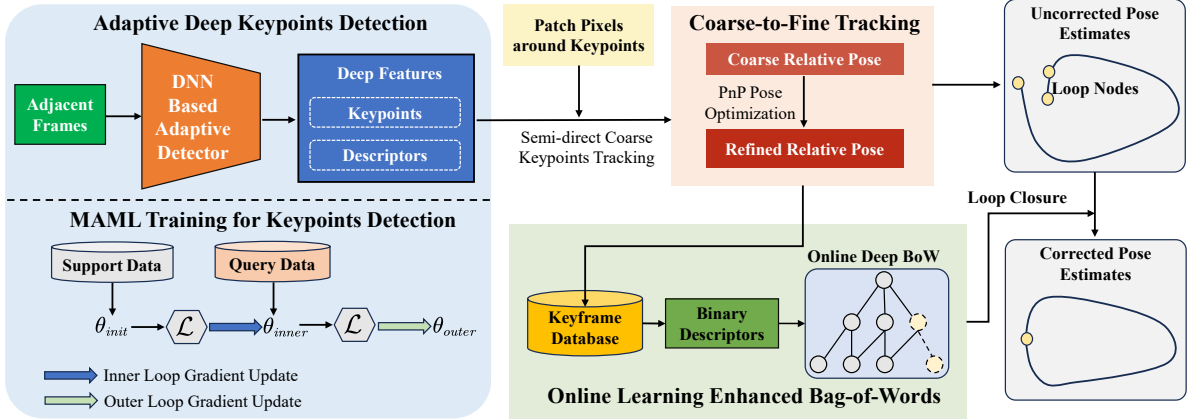


Fig. 1: An overview of our proposed DK-SLAM framework with adaptive keypoints, two-stage tracking and loop closure.

The descriptor loss L_d , illustrated in Equation 3 with z representing the boundary margin, is expressed as:

$$L_d = \frac{1}{N} \sum_{i=1}^N \max(0, z + L_{dm} - L_{dn}) \quad (3)$$

This descriptor loss L_d aims to minimize the feature distance between matching descriptors while maximizing the feature distance between non-matching descriptors. The overall training loss is the sum of the aforementioned detector loss and descriptor loss. Here, λ acts as a parameter to balance these different losses.

$$L_{\text{all}} = (L_p + L_{wp}) + \lambda L_d \quad (4)$$

3) *MAML for Feature Extractor Training*: Learning-based local feature extractors face poor generalization due to variances in visual features across scenes. Significant feature disparity between training and unseen datasets can lead to catastrophic forgetting. To address this, we leverage insights from Model-Agnostic Meta-Learning (MAML), adapting network parameters through meta-training for improved generalization and rapid adaptation to new data while preventing catastrophic forgetting. The MAML-based meta-training consists of inner loop training and outer loop training. The training set is partitioned into a support set \mathbf{D}_s and a query set \mathbf{D}_q , where \mathbf{D}_s is involved in inner loop training, and \mathbf{D}_q participates in outer loop training.

In the MAML training strategy, the original network parameter θ_a is initially duplicated to θ_b . Subsequently, both parameters undergo training in both the inner and outer loops. Within the inner loop, the support dataset \mathbf{D}_s is utilized for iterative updates to θ_b . This involves dividing a batch of support dataset into n distinct tasks τ , performing m parameter updates on each task. Consequently, within one inner loop, the parameters are updated $n * m$ times, resulting in the updated parameter θ_b^{n*m} . After completing one iteration of inner loop training, a complete batch of query set data is used to train the network. Although the gradient $\nabla_{\theta_b^{n*m}}$ is calculated for θ_b^{n*m} in the query set data, it is not used to update θ_b^{n*m} ; instead, the original θ_a is updated.

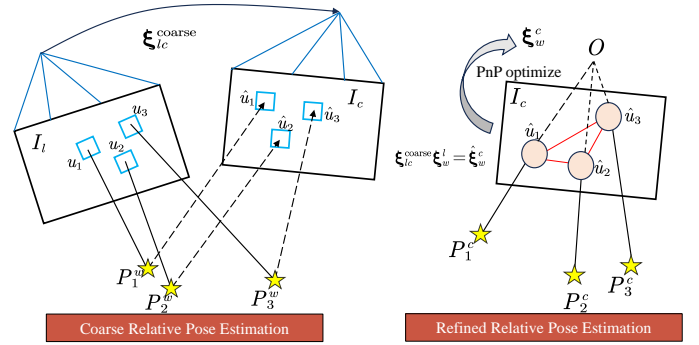


Fig. 2: A diagram of our proposed Coarse-to-Fine Tracking.

4) *Keypoint Distribution Strategy*: Furthermore, we incorporate a keypoint distribution strategy during the feature extraction stage. We uniformly distribute the entire set of keypoints across a multi-scale image pyramid. Within each layer of the image pyramid, a predefined number of keypoints is distributed evenly within the grid of different regions on the image. This distribution strategy ensures a balanced dispersion of keypoints across all scales and corners within an image, preventing concentration in specific areas.

B. Coarse-to-Fine Keypoint Matching and Tracking

Keypoint matching accuracy is crucial for visual SLAM performance. Traditional methods like ORB-SLAM use a motion tracking module based on adjacent frames, assuming a uniform motion model. However, this assumption often fails, leading to difficulties in finding correct matching correspondences and complicating the optimization process.

1) *Semi-direct Coarse Keypoint Tracking*: Taking inspiration from the semi-direct method [3], we introduce a coarse tracking method based on photometric constraints. We assume that the light intensity and texture around matching keypoints are similar in adjacent frames. Map points from the last frame are projected onto the current frame using the relative pose. If the relative pose is accurate, the photometric loss of the projected keypoint's patch will be minimal. As depicted in

equations 5 and 6, the pixels of the keypoint’s patch, the map points in the last frame coordinate \mathbf{p}_i^l , and the relative pose of adjacent frames ξ_{lc}^{coarse} collectively form the photometric loss L_p . Given the known map points and patch pixel values of the last frame, we adjust the relative pose ξ_{lc}^{coarse} to minimize the photometric loss L_p .

$$\xi_{lc}^{\text{coarse}} = \arg \min_{\xi_{lc}^{\text{coarse}}} \frac{1}{2} \sum_{i \in \bar{\chi}} \|L_p(\xi_{lc}^{\text{coarse}}, \mathbf{p}_i^l)\|^2 \quad (5)$$

$$L_p(\xi_{lc}^{\text{coarse}}, \mathbf{p}_i^l) = \mathbf{I}_c(\pi(\xi_{lc}^{\text{coarse}} \cdot \mathbf{p}_i^l)) - \mathbf{I}_l(\pi(\mathbf{p}_i^l)) \quad (6)$$

Here, π denotes the projection of the 3D map point from camera coordinates to pixel coordinates. $\bar{\chi}$ represents the set of keypoint indices. The photometric loss is constructed using the patches around the projected points.

2) *Coarse-to-Fine Keypoint Tracking*: Having obtained the coarse relative pose in the initial stage, we proceed to match map points between adjacent frames and refine the pose of the current frame ξ_w^c through the 3D-2D projection relationship. Subsequently, leveraging the coarse relative pose ξ_{lc}^{coarse} , we project the 3D map points from the last frame’s coordinate system to the pixel coordinate system of the current frame. Subsequently, we search for matching keypoints within a fixed radius range centered on the projection location, utilizing the Hamming distance of the descriptors as the search criterion.

Upon establishing the 3D-2D matching relationships, we construct a pose graph. As expressed in Equation 7, we employ the coarse relative pose in conjunction with the last frame’s pose to derive the initial pose of the current frame.

$$\hat{\xi}_w^c = \xi_{lc}^{\text{coarse}} \xi_w^l \quad (7)$$

The current frame’s pose serves as the vertex in the graph, with the number of vertices being subject to optimization. Map points from the current frame and the reprojection loss of these map points constitute the edges. We exclusively optimize the pose within the tracking module. As detailed in Equation 8, we iteratively refine the current frame pose $\hat{\xi}_w^c$ to minimize the reprojection loss. The g2o [30] framework is employed for optimizing the pose graph.

$$\xi_w^c = \arg \min_{\hat{\xi}_w^c} \frac{1}{2} \sum_{i \in \bar{\chi}} \|u_i - \pi(\hat{\xi}_w^c \cdot \mathbf{p}_i^w)\|^2 \quad (8)$$

C. Deep Keypoints based Loop Closing

Our DK-SLAM’s loop closure module includes detection and correction. To address poor generalization, we employ online learning-based Bag of Words (BoW) for the loop detector. Closed-loop nodes are identified, and the global map is optimized using the loop relative pose.

1) *Online learning based Binary Bow*: Unlike handcrafted descriptors, deep descriptors occupy a larger feature space. Offline-trained BoW models may struggle to capture this space, making it difficult to distinguish deep feature indices in BoW leaf nodes. To tackle this, we introduce an online learning-based BoW that uses features exclusively from testing scene data. Constructing a tree-like structure with floating

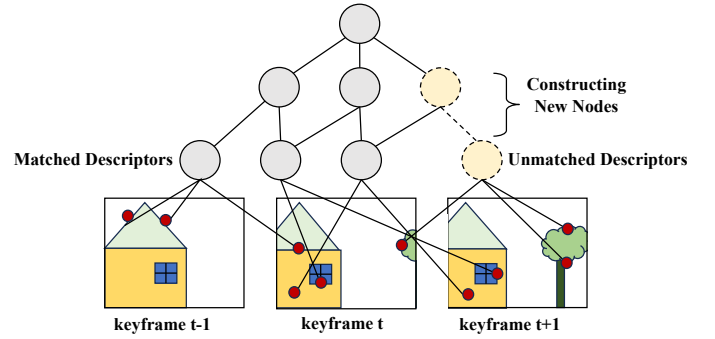


Fig. 3: Illustration of our proposed Online Learning based Binary BoW. The BoW is constructed incrementally, with matched descriptors in the keyframes database stored within the same leaf node. In the presence of unmatched descriptors in the current keyframe, a new leaf node is created.

descriptors is challenging, so, inspired by [31], we employ binary hash transformation for processing deep features. As depicted in Equation 9, for descriptor vector values \mathbf{d}_i less than 0, the processed $\hat{\mathbf{d}}_i$ is set to 0. For descriptor values greater than 0, the processed $\hat{\mathbf{d}}_i$ is set to 1, where i ranges from 0 to 256.

$$\hat{\mathbf{d}}_i = \begin{cases} 1 & \text{if } \mathbf{d}_i \geq 0 \\ 0 & \text{if } \mathbf{d}_i < 0 \end{cases} \quad (9)$$

2) *Loop Node Detection*: As shown in the Figure 3, the loop closure thread receives keyframes filtered from the local mapping thread, storing them in the inverted database to construct a Bag-of-Words (BoW). The iBoW-LCD utilizes the feature descriptors of the current frame K_c to match descriptors stored in the database. In iBoW-LCD, each keyframe is converted into a unique BoW vector for representation. We compute the similarity score between the current keyframe K_c and the BoW vectors of inverted keyframes to identify the most similar candidate keyframe K_h . However, the candidate keyframe K_h only considers differences in the numerical values of descriptors and neglects differences in descriptor positions, which may lead to mismatches.

Initially, we employ the Grid-Based Motion Statistics (GMS) [32] based brute force matching method to match keypoints between candidate closed-loop nodes. If the number of matches is below 20, the candidate loop keyframe is classified as a mismatch. GMS operates on the principle that the number of keypoints near correctly matched feature points should surpass the number near incorrectly matched keypoints. Following a procedure similar to ORB-SLAM2, we compute the similarity transformation matrix \mathbf{T}_{sim} between candidate closed-loop nodes through matched keypoints. Subsequently, \mathbf{T}_{sim} is applied to match map points between the current keyframe K_c and the candidate keyframe K_h . Further optimization of the similarity transformation matrix \mathbf{T}_{sim} is conducted using the matched map points. If the number of inliers in the optimization function exceeds 20, the candidate keyframe K_h is deemed a matched keyframe K_m .

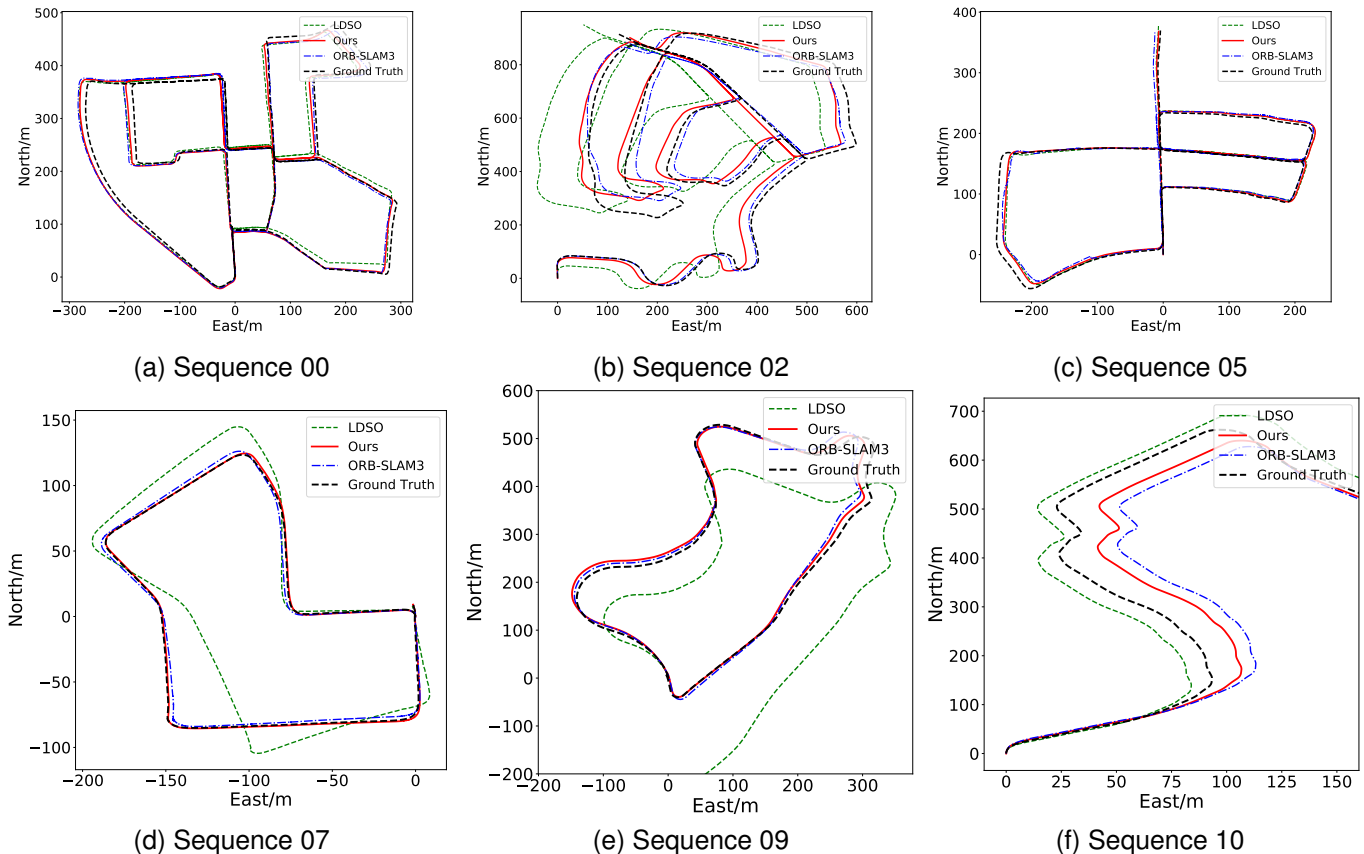


Fig. 4: The generated trajectories of our proposed DK-SLAM on the Sequence 00, 02, 05, 07, 09 and 10 of the KITTI dataset, comparing with LDSO and ORB-SLAM3.

3) *Global Map Correction by Loop Closure*: Optimizing the similarity transformation matrix \mathbf{T}_{sim} refines the pose of the current keyframe and its co-view related keyframes. Concurrently, we update the positions of co-observed map points across these keyframes. Next, we align the map points of the matched keyframe K_m and its connected keyframes with those of the current keyframe K_c and its connected keyframes. Updating the visibility graph between keyframes based on matched map points follows. Utilizing K_c , K_m , global map points, and the visibility graph, we construct and optimize the essential graph. Finally, a global bundle adjustment refines all keyframes and map point positions within the global map.

IV. EXPERIMENTS

A. Training Details and Datasets

1) *Training Details*: In MAML-based training, we set the batch size to 8, with 4 batches dedicated to support sets and 4 batches to query sets. Each minibatch is treated as a task, and 4 tasks are trained in the inner loop. The trained model calculates gradients on the query set, updating raw model parameters. The training spans 200k iterations, using the MSCOCO dataset [33].

2) *KITTI Odometry Dataset*: The KITTI odometry dataset [34] serves as a benchmark for self-driving scenarios, offering stereo RGB and grayscale images, along with Lidar and pose

ground truth data. Grayscale images from sequences 00, 02, 05, 07, 09, and 10 are utilized for pose evaluation.

3) *EuRoc MAV Dataset*: The EuRoc dataset [35] represents an indoor MAV flight dataset, encompassing stereo grayscale images, IMU data, and Leica Vicon’s pose ground truth. Grayscale images are collected at a frequency of 20Hz. Due to space limitations, we focus on sequences MH01-05 and V101 for SLAM performance evaluation.

B. Pose Evaluation on the KITTI Dataset

To assess our SLAM’s effectiveness, we experimented with the KITTI dataset using the official evaluation, computing root-mean-square error (RMSE) for translation and rotation vectors. The evaluation spanned sequences from 100m to 800m, providing an overall pose accuracy metric.

We thoroughly evaluated our SLAM’s tracking and loop closure in complex environments, focusing on KITTI’s 00, 02, 05, 07, 09, and 10 sequences. Pose estimation comparisons were made with LDSO [2], ORB-SLAM3 [12], VISO-M [36], and LIFT-SLAM [8]. VISO-M exhibited the lowest accuracy, facing failure scenarios, particularly in low-light conditions where corner detection proved unstable. LDSO, featuring a loop closure module, addressed accumulated errors in challenging scenes. ORB-SLAM3, an advanced keypoint-based SLAM with FAST corner detection and BRIFE descriptors,

TABLE I: The pose evaluation on the KITTI odometry dataset.

Method	Sensor	Metric	00	02	05	07	09	10	Avg
VISO-M	Mono	t_{rel}	36.95	21.98	17.20	20.00	29.01	28.52	25.61
		r_{rel}	2.42	1.22	3.52	5.30	1.32	3.23	2.84
LDSO	Mono	t_{rel}	2.84	4.91	2.07	12.76	23.14	9.20	9.15
		r_{rel}	0.36	0.74	0.24	5.13	0.21	0.21	1.15
ORB-SLAM3	Mono	t_{rel}	2.80	6.04	3.41	2.14	3.13	10.78	4.72
		r_{rel}	0.3	0.38	0.39	0.42	0.54	0.36	0.40
LIFT-SLAM	Mono	t_{rel}	3.18	8.73	6.09	2.42	19.91	9.72	8.34
		r_{rel}	2.99	2.49	3.11	4.02	2.14	2.24	2.83
Ours	Mono	t_{rel}	2.57	4.38	1.98	1.11	2.97	7.03	3.34
		r_{rel}	0.31	0.27	0.26	0.28	0.29	0.23	0.27

demonstrated exceptional performance across most scenes. Table I highlights ORB-SLAM3’s excellent performance in most sequences. However, a notable performance drop is observed in sequence 10, attributed to a lack of reliable corner points leading to unstable tracking and impacting overall pose estimation accuracy. Contrastingly, LIFT-SLAM, relying on learning-based local features, exhibits subpar performance across most sequences. This underscores that learning-based features may not universally surpass traditional features. ORB’s consideration of scale, direction, and a traditional SLAM technique for even keypoint distribution contribute to its competitive edge.

TABLE II: Comparison of absolute translation errors (in meters) between the proposed DK-SLAM and other baselines on the EuRoC dataset. Scaling with the ground truth is necessary for evaluation due to the absence of absolute scale in monocular visual SLAM methods, as noted in the table. ”-” indicates performance failure.

Method	MH01	MH02	MH03	MH04	MH05	Avg
DSO	0.046	0.046	0.172	3.810	0.110	0.8368
SVO	0.100	0.120	0.410	0.430	0.300	0.2720
DSM	0.039	0.036	0.055	0.057	0.067	0.0508
ORB-SLAM3	0.016	0.027	0.028	0.138	0.072	0.0562
LIFT-SLAM	0.044	0.053	0.049	-	-	-
Ours	0.013	0.013	0.027	0.077	0.055	0.0370

Learning-based local features perform well in matching benchmarks, but face challenges in SLAM due to correlated keypoints in dynamic scenes. Ignoring these correlations limits the exploitation of learning-based features’ advantages. Additionally, the feature space of learning-based features differs from handcrafted ones. Offline Bag-of-Words (BoWs) classify input features quickly, but traditional descriptors like BRIEF have a limited description space. Learning-based feature training is a ”black box,” complicating understanding, and testing performance depends on the training set’s distribution, hindering the acquisition of a generalized BoW.

Our proposed SLAM excels in most KITTI sequences, employing a coarse-to-fine matching strategy using keypoint-surrounding patches. Pose estimation optimization leverages

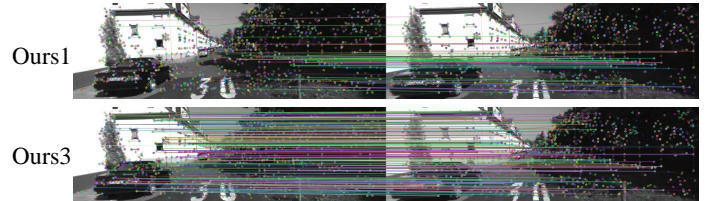


Fig. 5: The samples of keypoints detection and matching. Up: matching without two-stage strategy (Ours1). Bottom: matching with two-stage strategy (Ours3).

the 3D-2D matching relationship. Online training constructs a learning-based feature BoW using prior experienced data, limiting the BoW’s feature description space. Results confirm the online BoW’s effectiveness in loop scene detection, with the loop closure module accurately rectifying cumulative errors.

C. Pose Evaluation on the EuRoC Dataset

We validate our proposed DK-SLAM on the EuRoC dataset, addressing scale ambiguity with umeyama alignment [37] for monocular vision methods. Comparisons include ORB-SLAM3, DSO, DSM [38], SVO, and LIFE-SLAM [8]. Results, derived from [6] for ORB-SLAM3, DSO, DSM, and SVO, and [8] for LIFE-SLAM, utilize absolute translation error as the experiment metric. The proposed SLAM exhibits exceptional positioning performance, leveraging a two-stage tracking strategy for precise feature point location and reduced incorrect matching. Learnt features demonstrate robust detection in low-light environments, fostering stable feature tracking. The online learning-based deep BoW excels in loop detection, evident in MH02 where the proposed SLAM outperforms ORB-SLAM3. This advantage is attributed to learned features constructing BoW, providing detailed scene distinction, and online training for swift adaptation to varying environments.

D. Ablation Study

Table III summarizes the results of our ablation study, assessing the impact of our MAML-based deep feature training and coarse-to-fine feature tracking. In ”Ours1,” lacking a coarse-to-fine tracking strategy, reliance on a constant velocity

TABLE III: The ablation study into our DK-SLAM modules.

Method	MAML	Two-Stage	Metric	00	02	05	07	09	10	Avg
Ours1	✓		t_{rel}	2.88	-	2.80	1.76	2.70	-	-
			r_{rel}	0.41	-	0.35	0.64	0.24	-	-
Ours2		✓	t_{rel}	2.92	4.42	2.48	2.11	4.03	8.48	4.07
			r_{rel}	0.38	0.34	0.34	0.46	0.20	0.23	0.325
Ours3	✓	✓	t_{rel}	2.57	4.38	1.98	1.11	2.97	7.03	3.34
			r_{rel}	0.31	0.27	0.26	0.28	0.29	0.23	0.27

motion model for keypoint matching leads to errors, resulting in inaccurate correspondence and tracking failure. Both "Ours1" and "Ours3" use a keypoint search radius of 7.

Figure 5 shows a failure case for "Ours1" in accurate feature matching due to uniform motion model challenges. In contrast, "Ours3" uses a two-stage strategy for stable tracking, combining a semi-direct method for coarse pose estimation and refined feature matching. "Ours2" with the original Superpoint strategy performs slightly worse than "Ours3" trained with MAML. In "Ours3," MAML is applied to train the local feature extractor by iteratively enhancing generalization on support and query sets, resulting in a robust and adaptable detector. The enhanced SLAM performance attributed to MAML is primarily observed in feature matching, as depicted in Figure 6. Using Superpoints for matching increases the number of matches, addressing ORB-SLAM3's limitations in texture-less areas. ORB-SLAM3's descriptors, describing lighting changes around corners, are susceptible to environmental variations. In contrast, learning-based local feature methods like Superpoint capture robust deep features unaffected by lighting changes, ensuring stable tracking across consecutive frames.

Table IV presents the average number of matching points for ORB-SLAM3, Ours2, and Ours3 on Sequence 00, 05, 09, and 10 of the KITTI dataset. Setting the total number of keypoints to 3000 and pyramid level to 3, MAML-based training significantly improves the feature detection performance of superpoints, allowing them to acquire more robust features and enhancing SLAM accuracy.

TABLE IV: The average number of matching points for ORB-SLAM3, and DK-SLAM without (Ours2) or with MAML feature training (Ours3).

Seq	ORB-SLAM3	Ours2	Ours3
K00	228.3	352.6	376.7
K05	219.5	371.2	383.1
K09	150.4	258.0	265.3
K10	171.4	306.0	323.1

We perform ablation studies on the proposed loop closure method to assess its performance. Precision-Recall metrics on KITTI 00, 05, and 06 sequences are illustrated in Figure 7, with additional evaluation at 100% precision. The quantitative results, presented in Table V, reveal our deep BoW's superior recall rate compared to traditional BoWs. Notably, in the KITTI 06 sequence, our BoW achieves a remarkable

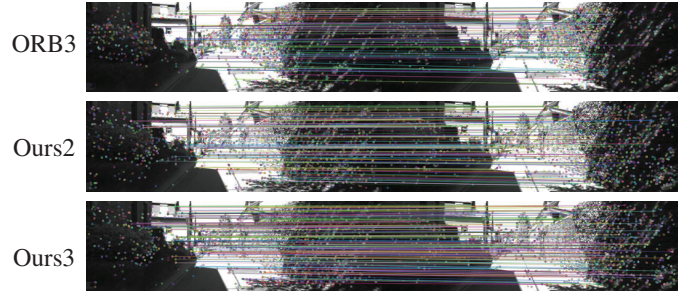


Fig. 6: The samples of keypoints detection and matching. From top to bottom: ORB-SLAM3 matching (ORB3), DK-SLAM without (Ours2) or with MAML feature training (Ours3).

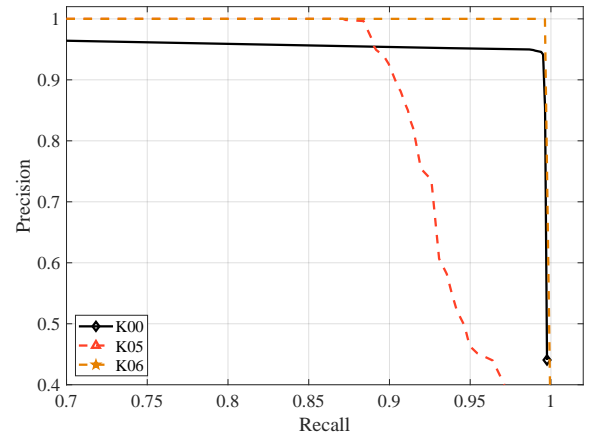


Fig. 7: Precision-Recall curves depicting the performance of the Bag-of-Words (BoW) approach in the proposed DK-SLAM on Sequences 00, 05, and 06 of the KITTI dataset.

TABLE V: Performance comparison of loop-closing with the maximum recalls across various methods, all achieving 100% precision. The numerical data presented in this table is sourced from [26], [39], and [40].

Seq	FAB-MAP2	Emilio	Milford	seqSLAM	iBoW	Ours
K00	0.49	0.90	0.67	0.67	0.77	0.98
K05	0.32	0.76	0.41	0.36	0.26	0.87
K06	0.55	0.95	0.65	0.65	0.96	1

100% recall rate. In contrast, the recall rate of the iBoW, belonging to the traditional BoW category, is significantly lower, suggesting that handcrafted descriptors might struggle

to accurately identify loop nodes in a sequence. The learned local descriptor captures high-level information, enhancing robustness across diverse environments. This feature stability, unaffected by lighting changes, results in superior loop detection performance.

V. CONCLUSION

This work presents DK-SLAM, a monocular visual SLAM with adaptive learning features, featuring a learned local feature detector, a coarse-to-fine matching strategy, and an online binary learned feature BoW. To enhance generalization, we employ MAML for adaptive training, yielding an extractor with robust capabilities. Coarse relative poses between frames are estimated via a semi-direct method for accurate feature point matching. An online binary learned feature BoW corrects SLAM accumulation errors. Our proposed DK-SLAM outperforms representative baselines, e.g. ORB-SLAM3, on the KITTI and EuRoC datasets. However, the GPU-based online front-end faces efficiency challenges during information transmission to the CPU-based back-end. Future work will explore knowledge distillation for parameter compression and SLAM framework modifications to enhance efficiency.

REFERENCES

- [1] J. J. Engel, V. Koltun, and D. Cremers, "Direct sparse odometry," *IEEE Transactions on Pattern Analysis and Machine Intelligence*, vol. 40, pp. 611–625, 2016.
- [2] X. Gao, R. Wang, N. Demmel, and D. Cremers, "Ldso: Direct sparse odometry with loop closure," in *2018 IEEE/RSJ International Conference on Intelligent Robots and Systems (IROS)*, 2018, pp. 2198–2204.
- [3] C. Forster, M. Pizzoli, and D. Scaramuzza, "Svo: Fast semi-direct monocular visual odometry," in *2014 IEEE International Conference on Robotics and Automation (ICRA)*, 2014, pp. 15–22.
- [4] R. Mur-Artal and J. D. Tardós, "Orb-slam2: An open-source slam system for monocular, stereo, and rgb-d cameras," *IEEE Transactions on Robotics*, vol. 33, no. 5, pp. 1255–1262, 2017.
- [5] C. Campos, R. Elvira, J. J. G. Rodríguez, J. M. M. Montiel, and J. D. Tardós, "Orb-slam3: An accurate open-source library for visual, visual-inertial, and multimap slam," *IEEE Transactions on Robotics*, vol. 37, no. 6, pp. 1874–1890, 2021.
- [6] Z. Teed and J. Deng, "Droid-slam: Deep visual slam for monocular, stereo, and rgb-d cameras," in *Neural Information Processing Systems*, 2021.
- [7] J. Tang, L. Ericson, J. Folkesson, and P. Jensfelt, "Gcnv2: Efficient correspondence prediction for real-time slam," *IEEE Robotics and Automation Letters*, vol. 4, pp. 3505–3512, 2019.
- [8] H. M. S. Bruno and E. Colombari, "Lift-slam: a deep-learning feature-based monocular visual slam method," *Neurocomputing*, vol. 455, pp. 97–110, 2020.
- [9] Y. S. Huaiyang Huang, Haoyang Ye and M. Liu, "Monocular visual odometry using learned repeatability and description," in *IEEE International Conference on Robotics and Automation (ICRA)*. IEEE, 2020.
- [10] Y. Lu and G. Lu, "Superthermal: Matching thermal as visible through thermal feature exploration," *IEEE Robotics and Automation Letters*, vol. 6, no. 2, pp. 2690–2697, 2021.
- [11] E. Rublee, V. Rabaud, K. Konolige, and G. Bradski, "Orb: An efficient alternative to sift or surf," in *2011 International Conference on Computer Vision*, 2011, pp. 2564–2571.
- [12] T. Lindeberg, *Scale Invariant Feature Transform*, 05 2012, vol. 7.
- [13] J. Shi and C. Tomasi, "Good features to track," *1994 Proceedings of IEEE Conference on Computer Vision and Pattern Recognition*, pp. 593–600, 1994.
- [14] T. Qin, P. Li, and S. Shen, "Vins-mono: A robust and versatile monocular visual-inertial state estimator," *IEEE Transactions on Robotics*, vol. 34, no. 4, pp. 1004–1020, 2018.
- [15] D. DeTone, T. Malisiewicz, and A. Rabinovich, "Superpoint: Self-supervised interest point detection and description," *2018 IEEE/CVF Conference on Computer Vision and Pattern Recognition Workshops (CVPRW)*, pp. 337–337 12, 2017.
- [16] M. Dusmanu, I. Rocco, T. Pajdla, M. Pollefeys, J. Sivic, A. Torii, and T. Sattler, "D2-net: A trainable cnn for joint description and detection of local features," in *2019 IEEE/CVF Conference on Computer Vision and Pattern Recognition (CVPR)*, 2019, pp. 8084–8093.
- [17] A. Barroso-Laguna and K. Mikolajczyk, "Key.net: Keypoint detection by handcrafted and learned cnn filters revisited," *IEEE Transactions on Pattern Analysis and Machine Intelligence*, vol. 45, no. 1, 2023.
- [18] Y. Tian, B. Fan, and F. Wu, "L2-net: Deep learning of discriminative patch descriptor in euclidean space," in *2017 IEEE Conference on Computer Vision and Pattern Recognition (CVPR)*, 2017.
- [19] J. Tang, J. Folkesson, and P. Jensfelt, "Geometric correspondence network for camera motion estimation," *IEEE Robotics and Automation Letters*, vol. 3, no. 2, pp. 1010–1017, 2018.
- [20] D. Li, X. Shi, Q. Long, S. Liu, W. Yang, F. Wang, Q. Wei, and F. Qiao, "Dxslam: A robust and efficient visual slam system with deep features," *2020 IEEE/RSJ International Conference on Intelligent Robots and Systems (IROS)*, pp. 4958–4965, 2020.
- [21] P.-E. Sarlin, C. Cadena, R. Siegwart, and M. Dymczyk, "From coarse to fine: Robust hierarchical localization at large scale," in *IEEE/CVF Conference on Computer Vision and Pattern Recognition (CVPR)*, 2019.
- [22] J. Jiang, X. Chen, W. Dai, Z. Gao, and Y. Zhang, "Thermal-inertial slam for the environments with challenging illumination," *IEEE Robotics and Automation Letters*, vol. 7, no. 4, pp. 8767–8774, 2022.
- [23] K. M. Yi, E. Trulls, V. Lepetit, and P. V. Fua, "Lift: Learned invariant feature transform," in *European Conference on Computer Vision*, 2016.
- [24] D. Galvez-López and J. D. Tardós, "Bags of binary words for fast place recognition in image sequences," *IEEE Transactions on Robotics*, vol. 28, no. 5, pp. 1188–1197, 2012.
- [25] M. Calonder, V. Lepetit, C. Strecha, and P. V. Fua, "Brief: Binary robust independent elementary features," in *European Conference on Computer Vision*, 2010.
- [26] E. Garcia-Fidalgo and A. Ortiz, "ibow-lcd: An appearance-based loop-closure detection approach using incremental bags of binary words," *IEEE Robotics and Automation Letters*, vol. 3, no. 4, 2018.
- [27] R. Arandjelović, P. Gronat, A. Torii, T. Pajdla, and J. Sivic, "Netvlad: Cnn architecture for weakly supervised place recognition," *IEEE Transactions on Pattern Analysis and Machine Intelligence*, 2018.
- [28] K. Simonyan and A. Zisserman, "Very deep convolutional networks for large-scale image recognition," *CoRR*, vol. abs/1409.1556, 2014.
- [29] Y.-Y. Jau, R. Zhu, H. Su, and M. Chandraker, "Deep keypoint-based camera pose estimation with geometric constraints," *2020 IEEE/RSJ International Conference on Intelligent Robots and Systems (IROS)*, pp. 4950–4957, 2020.
- [30] R. Kümmerle, G. Grisetti, H. Strasdat, K. Konolige, and W. Burgard, "G2o: A general framework for graph optimization," in *IEEE International Conference on Robotics and Automation*, 2011, pp. 3607–3613.
- [31] Y. Wang, B. Xu, W. Fan, and C. Xiang, "A robust and efficient loop closure detection approach for hybrid ground/aerial vehicles," *Drones*, vol. 7, no. 2, 2023.
- [32] J. Bian, W.-Y. Lin, Y. Matsushita, S.-K. Yeung, T.-D. Nguyen, and M.-M. Cheng, "Gms: Grid-based motion statistics for fast, ultra-robust feature correspondence," in *2017 IEEE Conference on Computer Vision and Pattern Recognition (CVPR)*, 2017, pp. 2828–2837.
- [33] T.-Y. Lin, M. Maire, S. J. Belongie, J. Hays, P. Perona, D. Ramanan, P. Dollár, and C. L. Zitnick, "Microsoft coco: Common objects in context," in *European Conference on Computer Vision*, 2014.
- [34] A. Geiger, P. Lenz, C. Stiller, and R. Urtasun, "Vision meets robotics: The kitti dataset," *The International Journal of Robotics Research*, vol. 32, pp. 1231 – 1237, 2013.
- [35] M. Burri, J. Nikolic, P. Gohl, T. Schneider, J. Rehder, S. Omari, M. Achtelik, and R. Y. Siegwart, "The euroc micro aerial vehicle datasets," *The International Journal of Robotics Research*, 2016.
- [36] A. Geiger, J. Ziegler, and C. Stiller, "Stereoscan: Dense 3d reconstruction in real-time," in *IEEE Intelligent Vehicles Symposium*, 2011.
- [37] S. Umeyama, "Least-squares estimation of transformation parameters between two point patterns," *IEEE Trans. Pattern Anal. Mach. Intell.*, vol. 13, pp. 376–380, 1991.
- [38] J. Zubizarreta, I. Aguinaga, and J. M. M. Montiel, "Direct sparse mapping," *IEEE Transactions on Robotics*, vol. 36, no. 4, 2020.
- [39] H. Yue, J. Miao, Y. Yu, W. Chen, and C. Wen, "Robust loop closure detection based on bag of superpoints and graph verification," in *2019 IEEE/RSJ International Conference on Intelligent Robots and Systems (IROS)*, 2019, pp. 3787–3793.
- [40] G. Singh, M. Wu, S. Lam, and D. Van Minh, "Hierarchical loop closure detection for long-term visual slam with semantic-geometric descriptors," in *2021 IEEE International Intelligent Transportation Systems Conference (ITSC)*, 2021, pp. 2909–2916.